Advances in Calcium Isotope Purification and Analysis Using Cutting-Edge Signal Amplifiers for Matrix-Diverse Reference Materials

Authors

Auguste Hassler[1,2,3,*], Eve E. Lindroos[1,4], Lu Yang[3], Anthony Dosseto[5], Florian Dux[5], Zoltan Mester[3], Kate Britton[2,‡], Clément P. Bataille[1,6,‡]

Affiliation

1: Department of Earth and Environmental Sciences, University of Ottawa, Advanced Research Complex building, 25 Templeton St., K1N 7N9, Ottawa, ON, Canada

2: Department of Archaeology, University of Aberdeen, St. Mary's Elphinstone Road, AB24 3UF Aberdeen, Scotland, UK

3: Metrology Research Centre, National Research Council Canada, 1200 Montreal Rd., Ottawa, Ontario, Canada K1A 0R6.

4: Géosciences Environnement Toulouse, Observatoire Midi Pyrénées, CNRS/UMR 5563, 14 avenue Edouard Belin, 31400 Toulouse, France

5: Wollongong Isotope Geochronology Laboratory, Environmental Futures, School of Science, University of Wollongong, NSW, 2522, Australia

6: Department of Forestry and Natural Resources, Purdue University, 715 W. State Street, West Lafayette, IN, 47907, USA

*: corresponding author

‡: These senior authors contributed equally

ORCID

Auguste Hassler: 0000-0003-3004-4680

Eve E. Lindroos: 0009-0004-8314-6685

Lu Yang: 0000-0002-6896-8603

Anthony Dosseto: 0000-0002-3575-0106

Florian Dux: 0000-0002-3275-710X

Zoltan Mester: 0000-0002-2377-2615

Kate Britton: 0000-0002-9478-5966

Clément Bataille: 0000-0001-8625-4658

Table of contents:

S1. Material and method supplements

S1.1 Column chromatography labware

In column chromatography with ion exchange resins, the quality of elemental separation and elution flow depends not only on the choice of resin and eluant, but also on the geometry of the column. The diameter of the resin bed controls the aspect ratio of the resin volume (i.e. diameter-to-height). For a given volume of resin, a smaller diameter yields a taller resin column, allowing for better elemental separation at the expense of a slower flow rate (Weiss, 2016). The elution flow rate is also influenced by the column aperture and frit properties (e.g. porosity, thickness), while the size of the column reservoir affects the workflow of chromatography operation, particularly in non-automated systems. Consequently, the optimal column geometry is application-specific, reflecting resin requirements and specifications, sample characteristics, and practical constraints. This is partly why in-house column manufacturing is common, though reliance on custom-made labware can hinder fast method transfer and reproducibility.

For the chromatography procedure described in this study, columns selected are readily available and accessible to laboratories worldwide. The method builds on Tacail et al. (2014) but was redesigned using Poly-Prep® Chromatography Columns (polypropylene, 2 ml bed volume, 10 ml reservoir, 0.8 cm bed diameter, Bio-Rad) for the first chromatography steps (with AG® 50W-X12 and AG® 1-X8 resins). For the final strontium–calcium separation (using Sr resin, Eichrom), we adapted polyethylene transfer pipets (Polyethylene, #134070, 5 ml native volume, 0.46 cm stem diameter used as resin bed, Globe Scientific Inc), a good compromise of practicality and sample throughput (appropriately large 10 ml reservoir, resin bed diameter large enough to limit bubble formation), which provide a more favorable resin bed aspect ratio (i.e. smaller diameter, taller resin bed). To prepare these custom columns, the pipette tip and bulb top were cut away, leaving a 2.5 cm long (0.46 cm in diameter) stem to serve as the resin bed, yielding a total capacity of ~4 ml including the bulb. A polyethylene frit of 1.6 mm (medium porosity, H13638-5116, Bel-Art) was trimmed to slightly larger than the stem diameter and inserted at the bottom of the column to retain the resin (300 µL of 50-100 µm particle size Sr resin, Eichrom).

S1.2 Additional labware and consumables

Unless otherwise specified, all tested materials were processed in Perfluoroalkoxy alkanes (PFA) vials (#200-007-20, #200-015-20, Savilex) from digestion (apart from microwave digested material) through transfer into autosampler compatible vials for analysis. For microwave assisted acid digestion (Anton Paar system), polytetrafluoroethylene (PTFE) vials were used (PTFE-TFM, #179047, Anton Paar). Polypropylene consumables included metal free centrifuge tubes (15 ml and 50 ml, MetalFree, Labcon) and pipette tips (200 µl yellow, 1000 µl blue, 5 ml transparent, Vertex). Polyethylene consumables included LDPE autosampler vials (2.5 ml with hinged cap, Fisherbrand).

S1.3 Labware cleaning procedures

Perfluoroalkoxy alkanes (PFA) vials were cleaned using a 3-step protocol: sequential 48 h soakings in 5M HCl and then 7.5M HNO_3 (both ACS grade) at 120°C, followed by 1 h in boiling 7.5M TMG HNO_3 at 120°C. Three milli-Q rinses were performed before and after each step. Polytetrafluoroethylene (PTFE) vials used for microwave digestion (Multiwave 7000, Anton Paar system) were cleaned by a 2-step protocol consisting of two successive organic-high digestion runs (20 min ramping, 15 minutes holding at 250°C, starting pressure 40 bar) with 1ml of 15M HNO_3 (ACS and with three milli-Q rinses before and after each step. Polypropylene and low-density polyethylene consumables were cleaned by a 2-step protocol: 48 h soakings in 2M HCl (ACS) and then 3M TMG HNO_3 at ambient temperature, with three milli-Q rinses performed before and after each step. After cleaning, all consumables were dried under a laminar flow hood in a Class 1000 clean laboratory.

S1.4 Resin reuse and cleaning procedures

Prior to first use, AG® 1-X8 resin (100-200 mesh, Bio-Rad) was cleaned through successive steps of mixing with diluted TMG HNO_3 0.5 M, and TMG HCl 6 M, separated by triple rinses with ultrapure water. Each acid cleaning step was repeated at least twice, and until the supernatant after settling was colorless. After the resin was transferred to columns, a routine wash was performed before each use. This sequence consisted of successively loading ~10 ml of: H_2O → HNO_3 0.5 M → H_2O → HCl 6 M → H_2O (all ultrapure or TMG grade). Each solution was loaded only after complete elution of the previous one.

Prior to first use, AG® 50W-X12 resin (200-400 mesh, Bio-Rad) was cleaned through successive steps of mixing with diluted TMG HCl 6 M, separated by triple rinses with ultrapure water. The HCl cleaning step was repeated at least three times, and until resulting rinses were colorless. After the resin was transferred to columns, a routine wash sequence was performed before each use. For columns loaded with 1 ml of resin, the wash sequence consisted of successively loading ~10 ml of: HCl 6 M → H_2O → HCl 6 M. For columns loaded with 2 ml of resin, the sequence consisted of successively loading ~5 ml of: HCl 6 M → H_2O, followed by two ~10ml of HCl 6 M. All these washes were done using ultrapure or TMG grade solutions with each step applied only after complete elution of the previous one.

After use and following the terminal wash step of the relevant chromatography procedure (see main text), both these resins (AG® 1-X8, and AG® 50W-X12) were stored in the same columns used for chromatography. Columns were sealed in acid cleaned metal-free 50 ml polypropylene tubes (Labcon) filled with ultrapure water up to the top level of the resin bed. Under these conditions, AG® 1-X8 was successfully reused up to ~5 times, and AG® 50W-X12 up to ~15 times, over 6-month periods without noticeable aging (e.g. elevated blanks, reduced yields, or Ca isotopic fractionation in secondary standards).

Sr resin (Eichrom) used for Ca-Sr separation was prepared by slurrying in 0.005 M HNO_3 (TMG) and storing overnight in a fridge. Columns were packed with this resin on the day Ca-Sr separation, then routinely washed by two sequential washes with ~4 ml of 0.005 M HNO_3 (TMG). Within this study, the Sr resin was used only once per separation, and no reuse was attempted.

S1.4 Chromatography step designs

The branching chromatography procedure presented in this study derives from previously established methods (Guiserix et al., 2022; Lamboux et al., 2020; Le Goff et al., 2021; Tacail et al., 2014).

Step 0.

The elimination of Fe, Cu and Zn from the Ca fraction (step 0., Table 1) was performed using 2 ml of AG® 1-X8 resin (100-200 mesh, Bio-Rad) and followed the procedures described in (Le Goff et al., 2021; Tacail et al., 2014), with the only major modification being the use of a large loading volume (3.5 ml, equivalent to 175% of the resin volume). This likely induces peak widening but was necessary to properly dissolve large sample amounts from Ca poor samples (representing up to 91 mg pre-digestion). It was demonstrated that this adaptation did not compromise the quality of the Fe and Cu separation from the Ca fraction and the remaining matrix (Figure 1). Step 0. typically requires 4-5 hours to complete, including wash sequence.

Step 1a.

The aim of step 1a (Table 1) is to separate Ca and Sr fractions from most of the elemental matrix in high Ca/matrix samples, using 1 ml of AG® 50W-X12 resin (200-400 mesh, Bio-Rad) in Bio-Rad PP columns. This procedure was adapted from Lamboux et al., 2020; Tacail et al., 2014. The relatively large resin bed diameter helps preventing bubble formation during the chromatography and is convenient due to the generous large reservoir volume and fast flow frit. However, the large diameter of 0.8 cm also results in a relatively poor aspect ratio (i.e. height/diameter of the resin bed). Elutions with smaller resin volumes (0.25-0.5 ml) were tested but proved unsatisfactory for routine sample sizes (e.g. ≥ 0.5 mg of dry mass pre-digestion for bones). These tests showed partial overlap of Mg or K with the Ca elution peak and increased difficulty in preventing mobilization of relatively large resin fraction during reagent loading, which reduced reproducibility across samples. Although small Mg or K carryover may not significantly affect Ca isotope measurements depending on MC-ICP-MS setup and associated thresholds (see doping experiments in Bao et al., 2020; Hassler, 2021 and this study), reliability was improved by increasing the resin volume. For high Ca/matrix samples, using 1 mL of resin represented the best compromise between resin/acid consumption and robustness of element separation. Step 1a typically requires ~7 hours to complete, including wash sequence.

Step 1b.

Lower Ca/matrix samples (e.g., seawater or soft tissues) and samples with higher K or Mg content required more resin to achieve a satisfactory separation of Ca and Sr fractions from the remaining elements (step 1b., Table 1). Using 2 ml of AG® 50W-X12 resin (200-400 mesh, Bio-Rad), similarly to Le Goff et al., 2021; Tacail et al., 2014, was found to provide reliable performance for the tested materials. For DOLT-5, slight K peak tailing overlapping with the Ca fraction was identified when only 55 mL of 1 M HCl was used for sample loading and matrix elution, leading

to contamination of the Ca fraction with 1 to 2 ng of K. Although doping experiments confirmed that this amount of K does not affect Ca isotope measurements, the total elution volume was increased to 60 ml (as displayed in Table 1). This adjustment further reduced the risk of K carryover, notably for samples with higher K than DOLT-5, while maintaining full Ca yields. Step 1b typically requires ~11 hours to complete, including wash sequence.

Step 2.

Finally, the separation of Sr from Ca (step 2., Table 1) using Sr resin from Eichrom was only marginally modified from the protocol described in Guiserix et al., 2022, and earlier works like Tacail et al., 2014. Despite using resin volumes (0.3 ml) with a Sr retention capacity far exceeding maximum loaded Sr amounts (1 µg) and working with Ca molarities (< 5.10^{-5} M) well below levels known to affect Sr affinity with the resin (Horwitz et al., 1992), it was observed that Sr resin with a 100-150 µm particle size (such as used in Guiserix et al., 2022; Tacail et al., 2014) leaved small fractions of Sr seeping through the resin and contaminating the Ca fraction. For loads of 1 µg of Sr and 50 µg of Ca in 3 M HNO3 (TMG), collected Ca fractions contained 30 to 200 ng of Sr (3 to 20% of the loaded Sr), levels sufficient to compromise most Ca isotope measurements by MC-ICP-MS (see Figure 4). Two batches of this resin grade (purchased respectively more than 6 months and just before the tests) were tested in parallel and provided variable but consistently high Sr contaminations. Tests with larger resin volumes (0.5 and 0.75 ml; corresponding to 5.5 and 7.5 ml of 3 M HNO3 (TMG) for Ca collection) achieved smaller but very inconsistent Sr contaminations (0.07 to 36 ng of Sr, mean= 17.44 ng, n = 2 per resin volume). During the same chromatography session, 0.3 ml of Sr resin with 50-100 µm particle size, tested under the same elution procedure, yielded reproducibly low Sr contamination (0.3 ng in the Ca fraction). Our hypothesis is that the 100-150 µm resin grade can sometime form micro gaps of porosity within the resin bed or at the interface between the resin and the column. This can limit the interaction between the resin and the liquid phase, in worst cases forming micro channels where some of the Sr can bypass some of the resin. This may explain occasional Sr contamination in some Ca isotope measurement routines using similar methodologies. A more thorough resin packing (deposited by simple gravity sedimentation in our case) or picking columns with a better aspect ratio (higher length over diameter ratio of the resin bed) may reduce such Sr micro leaks in the 100-150 µm particle size Sr resins. We hypothesize that the better performance and the superior reliability of the 50-100 µm particle size Sr resin likely reflects its more cohesive packing, which visibly reduces porosity. This grade Sr resin also simplifies resin loading workflow, though at the cost of a significantly slower flow rate—processing time per batch increased by ~1.75× compared to the 100–150 µm resin. Step 2 typically takes ~10 h to complete with 50-100 µm particle size resin, including column loading and wash sequence.

S1.5 Routine ICP-MS setting tuning

Example of routine settings, in wet plasma RF 1200 W, with H cone configuration and hybrid amplifier association (2x $10^{11}\Omega$, 2x $10^{13}\Omega$), the system was tuned using an alpha-Ottawa solution at 10 ppm of Ca in 2% HNO3 v/v (screenshots from Multicollector Software Version 3.2.1.15, Thermo Fisher Scientific, analytical session 30/10/2024):

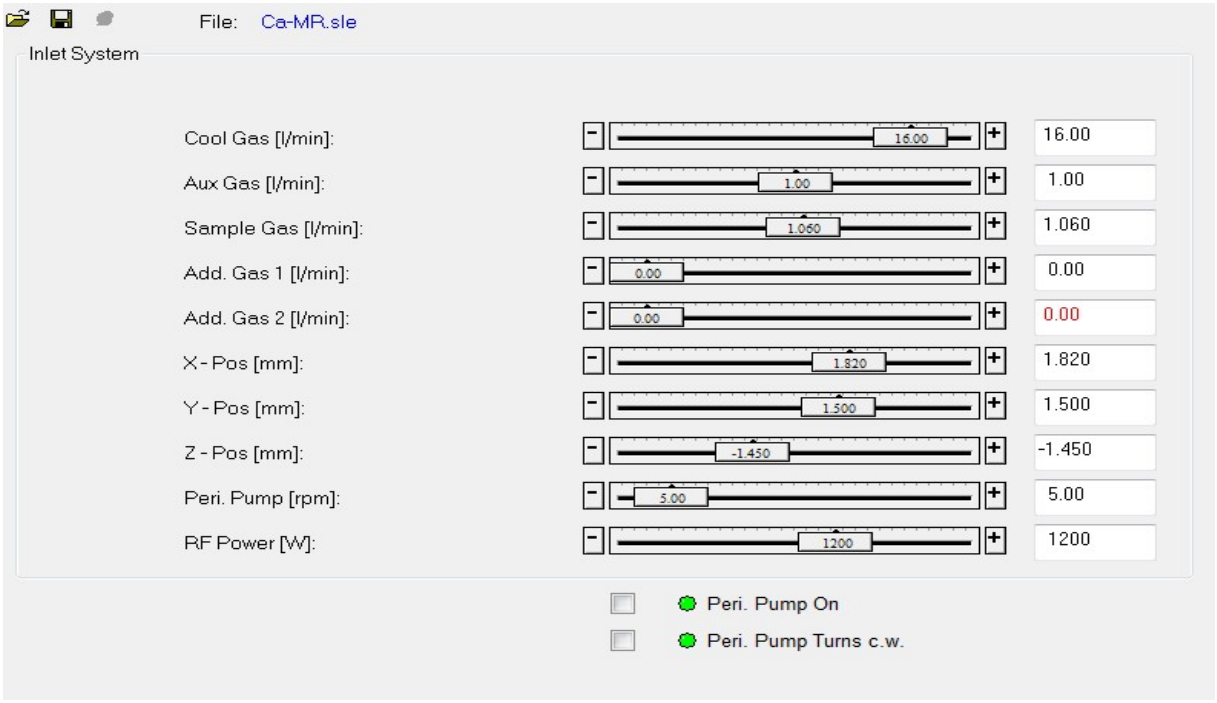

Figure S1.5A
Inlet system screenshot.

Notes:

- Sample Gas was tuned for each nebulizer, auto-sampler probe tubing and cyclonic chamber combination to optimize ionic transmission and stability.
- Torch position (particularly X and Y) was tuned after each cone replacement to optimize ionic transmission and stability. More frequent tuning has rarely provided further benefits.

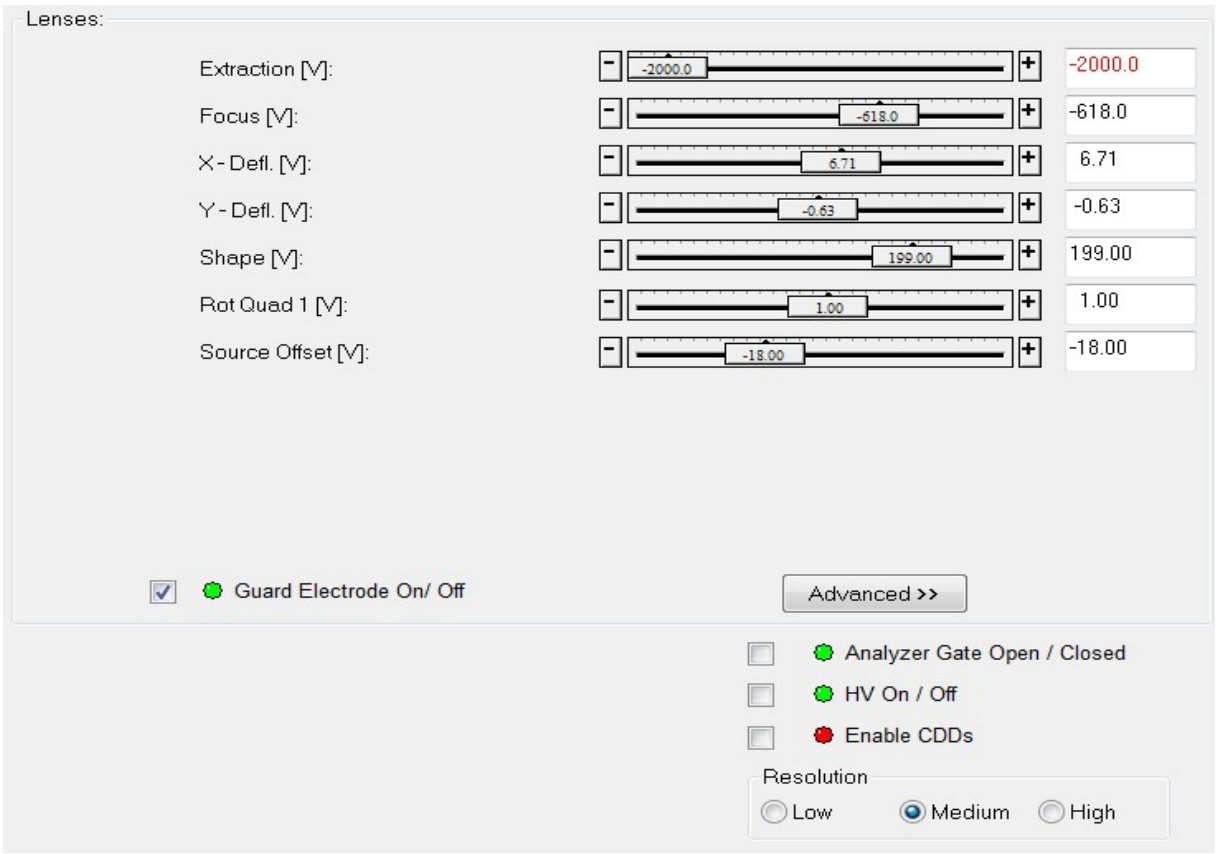

Figure S1.5B
Source lenses screenshot.

Notes:

- Focus, X-Defl., Y-Defl. and Shape were regularly tuned in between series or single analytical sessions to optimize ionic transmission and stability.

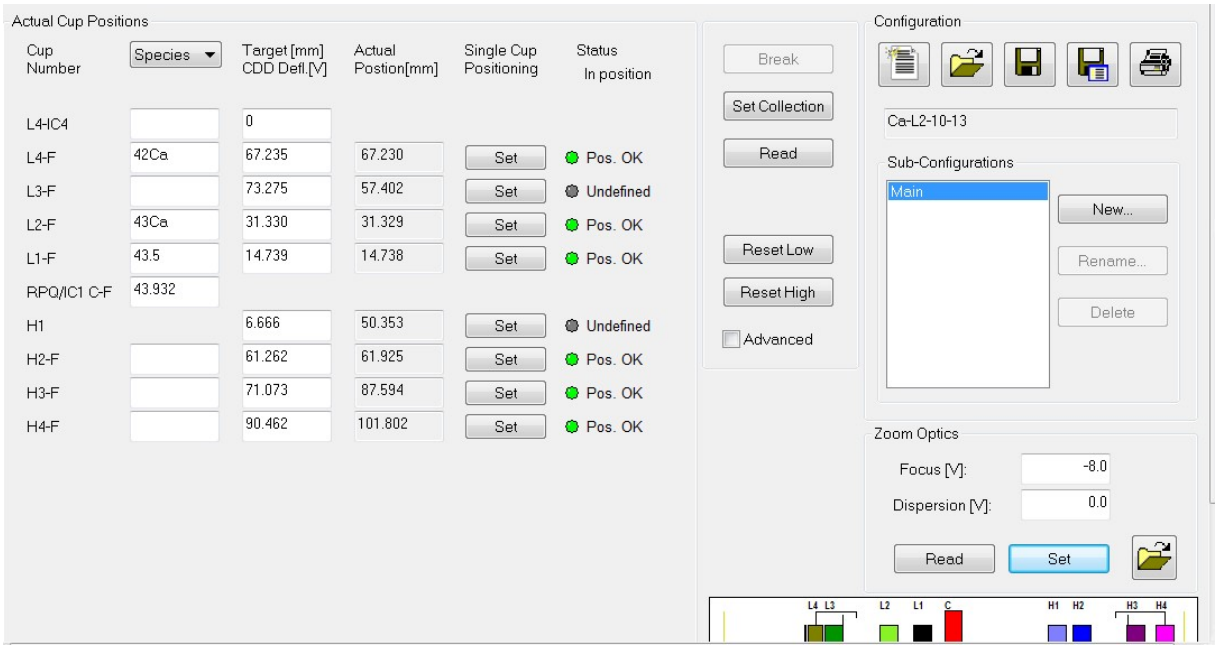

Figure S1.5C
Cup configuration screenshot.

Notes:

- Besides central cup (C), cup positions were left unchanged past initial fine-tuned alignment.
- Optics focus was tuned along with the MR slit progressive wear to maintain narrow “discrete” magnetic field plateaux.

Resulting 0.1s integration 100 step mass scan:

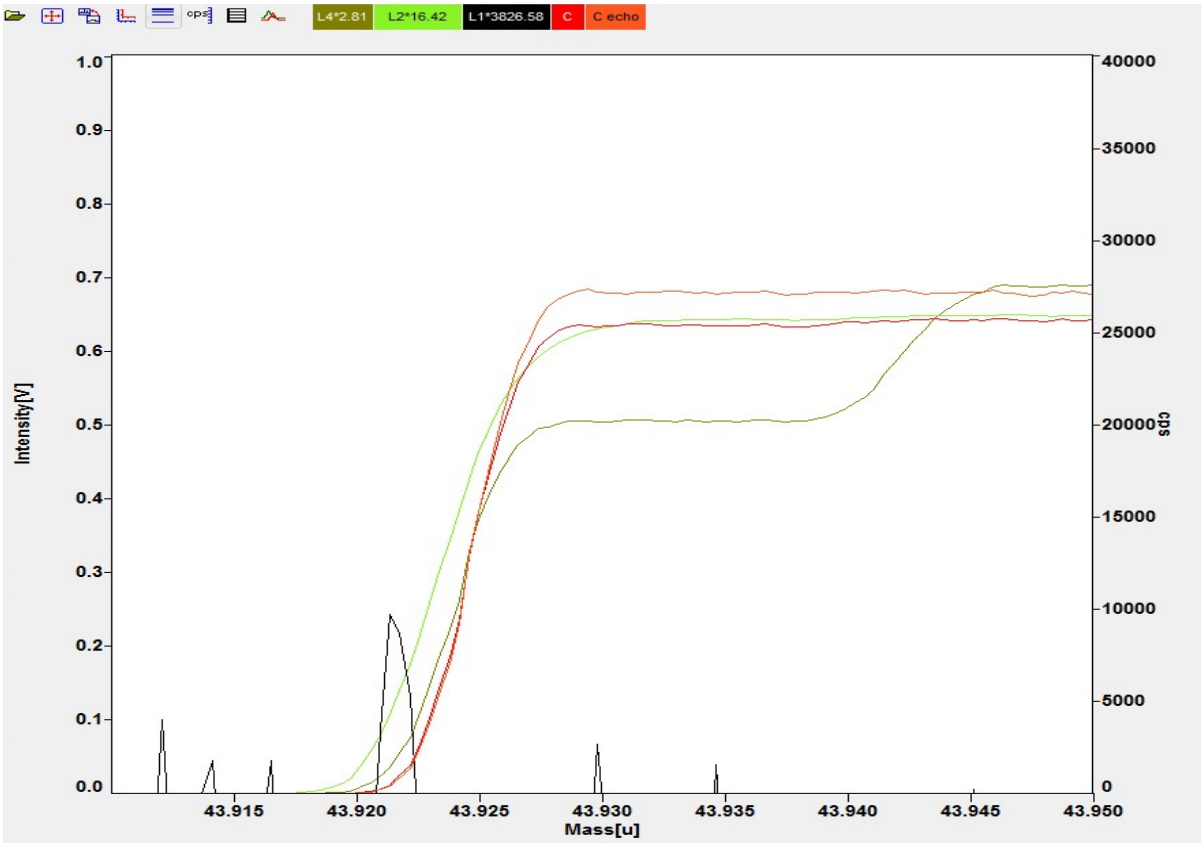

Figure S1.5D
Mass scan screenshot.

Notes:

- With the exception of the central cup (C), cup positions were left unchanged past initial fine-tuned alignment as signal alignment has stayed consistent over time (> 1 year of observation).
- Optics focus was tuned over time to account for MR slit progressive wear, ensuring narrow, "discrete" magnetic field plateaux.
- Reported intensity values incorporate gain calibration factors (close to 1 for $10^{11}\Omega$ amplifiers, and close to 0.01 for $10^{13}\Omega$ amplifiers) and plot specific multipliers (top legend), applied to facilitate visualization of signal alignment.
- L4 double plateaux illustrate $^{42}Ca^{2+}$, $^{40}ArH_2^+$-free signal (left plateau) and the $^{42}Ca^{2+}$ + $^{40}ArH_2^+$ signal (right plateau, > 43.938 u).
- The apparent misalignment of the L2 cup (paired to a $10^{13}\Omega$ amplifier here) is simply an artifact resulting from the 0.1s integration time used for the mass scan and the behavior of $10^{13}\Omega$ amplifiers. Using longer integration time (e.g. 4.194 s) demonstrates appropriate alignment.
- The alpha-Ottawa solution contains only pico-traces of Sr after step 2 chromatography. L1 record here is therefore only highly amplified noise. Cup alignment for L1 was established during a previous analytical session using a Sr bearing solution. Note that Sr^{2+} ion beam positions do not exactly match corresponding Ca^+ ion beam positions.
- C echo is a record from the previous analytical session released about 15 hours prior. It illustrates the common trend of slow decrease of signal intensity over day periods (plateauing at about - 0.2 V from day 1 maximum). This loss is fully reset after periods with the instrument cooling-off (hours to days). Part of this loss can be linked to cone progressive clogging, but this factor was observed to have only a minimal impact at this time scale in the presented analytical configuration.
- An interference was identified on the L4 cup between 43.9281 and 43.930 u that is not visible in the mass scan. More details about this interference are provided in the following section.

S1.6 Report on unusual "ghost" $^{42}Ca^+$ interference

Over the course of multiple analytical sessions, a peculiar $^{42}Ca^+$ interference was detected. Although this interference was easily avoided and therefore did not significantly impact the present study, it could potentially impact Ca isotope measurements on other instruments (whether using the present methodology or alternative approaches) and was thus deemed worth reporting. While its exact cause remains unknown, its behavior was closely studied which allows to draw general guidelines for monitoring and avoiding it.

This interference manifested as an excess signal at mass 42 (L4), measuring ~+0.2 V in H cone configuration and ~+1.8V in X cone configuration. It appeared precisely and invariably between 43.9281 and 43.930 u of the magnetic field relative to the fixed axial detector. This interference was observed during both blank and Ca solution introduction. It remained confined to this above-mentioned mass range regardless of cup position or adjustments to routine parameters. Notably, this interference was only visible during discrete magnetic field position scans (i.e., set scan in Tune software) and during data acquisition (via Method or Sequence editors). It was never visible in mass scans regardless of tested parameters (various resolutions and integration times, see example in previous section). For this reason, it was informally referred to as the "ghost" interference. This interference was consistently observed for more than a year with unchanged characteristics and, if not avoided, led to clear outliers in measured Ca isotopic compositions. However, it was straightforward to mitigate by either avoiding the affected range of the magnetic field or by adjusting cup positions to move targeted signals away from the interference. The nature of this interference is unknown, unlike any expected or typical elemental or spectroscopic interference, and we suggest it may have arisen from software or hardware artifacts.

S1.7 Intensity match

Differences in Ca concentration between samples and bracketing standards are known to bias Ca isotope measurements (e.g., Bao et al., 2020). However, our tests on all seven secondary standards (Figure S1) demonstrate that no systematic bias in $\delta^{44/42}Ca$ values was observed within our routine concentration match range of ± 10 % between samples and bracketing standards (n = 417).

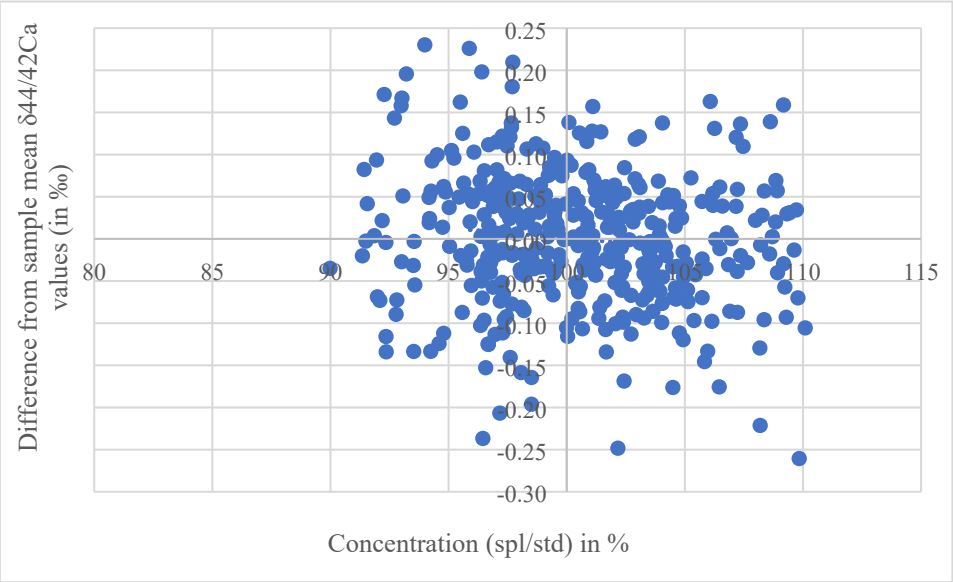

Figure S1.7A
Plot of all measured secondary standard $\delta^{44/42}Ca$ values (n= 417) subtracted by the average value of the corresponding secondary standard (in ‰, y axis, mean values from this study) in function of the relative signal intensity of $^{44}Ca+$ for the measurement compared to bracketing standard measurements (in %, x axis).

S1.8 Implementing Sr^{2+} correction

Sr^{2+} correction formulas (e.g., for $^{42}Ca^{+}$: $V_{42\text{-}c} = V_{42} - V_{43.5} \times R_{87/84} \times (M^{84}Sr / M^{87}Sr)^{f}$, see main text for $^{43}Ca^{+}$ example and formula detailed description) can either be applied within the Neptune software (method editor) or offline during data processing via Excel, with no significant difference in resulting $\delta^{44/42}Ca$ values. However, corrected $\delta^{43/42}Ca$ and $\delta^{44/43}Ca$ values calculated offline in Excel were on average closer to the theoretical 0 ‰ for alpha-Ottawa standards bracketed on themselves (closer for about 75% of cases), potentially because of differences in decimal processing between softwares. Consequently, the offline correction method was preferred in this study.

Supporting tables S2 to S5

Included in a separated appendix as an excel file.

Supplementary information bibliography

(excluding supporting table S3 self-contained bibliography)

Bao, Z., Zong, C., Chen, K., Lv, N., & Yuan, H. (2020). Chromatographic purification of Ca and Mg from biological and geological samples for isotope analysis by MC-ICP-MS. *International Journal of Mass Spectrometry*, *448*, 116268. https://doi.org/10.1016/j.ijms.2019.116268

Guiserix, D., Albalat, E., Ueckermann, H., Davechand, P., Iaccheri, L. M., Bybee, G., Badenhorst, S., & Balter, V. (2022). Simultaneous analysis of stable and radiogenic strontium isotopes in reference materials, plants and modern tooth enamel. *Chemical Geology*, *606*, 121000. https://doi.org/10.1016/j.chemgeo.2022.121000

Hassler, A. (2021). *Mammalian reproduction strategies and calcium isotopes: modern evidence and deep-time perspectives*. Ecole normale supérieure de Lyon, University of Lyon.

Horwitz, E. P., Chiarizia, R., & Dietz, M. L. (1992). A novel strontium-selective extraction chromatographic resin. *Solvent Extraction and Ion Exchange*, *10*(2), 313–336. https://doi.org/10.1080/07366299208918107

Lamboux, A., Hassler, A., Davechand, P., & Balter, V. (2020). Absence of temperature effect on elution profiles on anionic and cationic ion-exchange resins from 4°C to 28°C. *Rapid Communications in Mass Spectrometry*, *34*(13), e8806. https://doi.org/10.1002/rcm.8806

Le Goff, S., Albalat, E., Dosseto, A., Godin, J., & Balter, V. (2021). Determination of magnesium isotopic ratios of biological reference materials via multi-collector inductively coupled plasma mass spectrometry. *Rapid Communications in Mass Spectrometry*, *35*(10). https://doi.org/10.1002/rcm.9074

Tacail, T., Albalat, E., Télouk, P., & Balter, V. (2014). A simplified protocol for measurement of Ca isotopes in biological samples. *Journal of Analytical Atomic Spectrometry*, *29*(3), 529–535. https://doi.org/10.1039/c3ja50337b

Weiss, J. (2016). *Handbook of Ion Chromatography* (4th ed., Vols. 1, 2, 3). John Wiley & Sons.